

PROCEEDINGS OF SPIE

[SPIDigitalLibrary.org/conference-proceedings-of-spie](https://spiedigitallibrary.org/conference-proceedings-of-spie)

The detection of objects in a turbid underwater medium using orbital angular momentum (OAM)

Brandon Cochenour
Lila Rodgers
Alan Laux
Linda Mullen
Kaitlyn Morgan
Jerome K. Miller
Eric G. Johnson

The detection of objects in a turbid underwater medium using orbital angular momentum (OAM)

Brandon Cochenour, Lila Rodgers, Alan Laux, Linda Mullen, Kaitlyn Morgan, Jerome K. Miller, Eric G. Johnson

1 - Naval Air Warfare Center, 22347 Cedar Point Rd, Patuxent River MD 20670, USA

2 - Micro-Photonics Laboratory, Center for Optical Materials Science and Engineering Technologies, Holcombe Department of Electrical and Computer Engineering, Clemson University, 315 Riggs Hall, Clemson SC, 29634

ABSTRACT

We present an investigation of the optical property of orbital angular momentum (OAM) for use in the detection of objects obscured by a turbid underwater channel. In our experiment, a target is illuminated by a Gaussian beam. An optical vortex is formed by passing the object-reflected and backscattered light through a diffractive spiral phase plate at the receiver, which allows for the spatial separation of coherent and non-coherent light. This provides a method for discriminating target from environment. Initial laboratory results show that the ballistic target return can be detected 2-3 orders of magnitude below the backscatter clutter level. Furthermore, the detection of this coherent component is accomplished with the use of a complicated optical heterodyning scheme. The results suggest new optical sensing techniques for underwater imaging or LIDAR.

Keywords: Underwater, backscattering, orbital angular momentum, OAM

1. INTRODUCTION

Orbital angular momentum (OAM) is a property of light describing the helicity of the optical phase front. A vector normal to the wavefront (i.e. the Poynting vector) possesses an azimuthal component which causes the vector to twist around the beam axis. This helical nature creates a phase discontinuity in the center of the beam, resulting in a so-called optical vortex. Allen et. al.¹ noted that any helically phased beam carries OAM, with a phase component described by $\exp(-jm\phi)$, where ϕ is the azimuth angle, and m is the azimuthal mode index, or charge number of the beam. The charge describes the number of 2π phase rotations of the phase front upon propagating a distance of one wavelength, and can be positive or negative depending on the direction of rotation.

The use of OAM underwater has only recently be considered, mainly for the purpose of increasing the bandwidth capacity of wireless optical communication links by multiplexing several OAM orders together.^{2,3} For this reason, experiments investigating the propagation behavior of forward scattered light with beams carrying OAM have been performed.⁴

The dependency between optical coherency and the formation of an optical vortex can potentially be exploited in a number of interesting ways for optical remote sensing. Sun et. al. has proposed using OAM as a method for solar background rejection in airborne LIDAR systems,⁵ where the optical vortex can be used to spatially separate incoherent solar ambient from coherent object returns. This is a similar motivation in the astronomy community, which has used OAM to create optical chronographs.^{6,7} Palacios⁸ described an experiment that used a diffractive spiral phase plate⁹ as an ‘analyzer’ to study the relationship between ballistic and forward scattered light. They noted that while both the ballistic (coherent) and scattered (non-coherent) light passes through the phase plate, a helical phase is imparted only upon the coherent ballistic photons. Therefore, the optical vortex and its hollow core can be considered a ‘window’ for spatially separating non-scattered and scattered light.

The desire to separate scattered from non-scattered (or coherent from incoherent) is common in ‘backwards’ geometries such as imaging or LIDAR where the challenge is to detect a target obscured in an optically thick

Corresponding author information:

B.M.C.: E-mail: brandon.cochenour@navy.mil

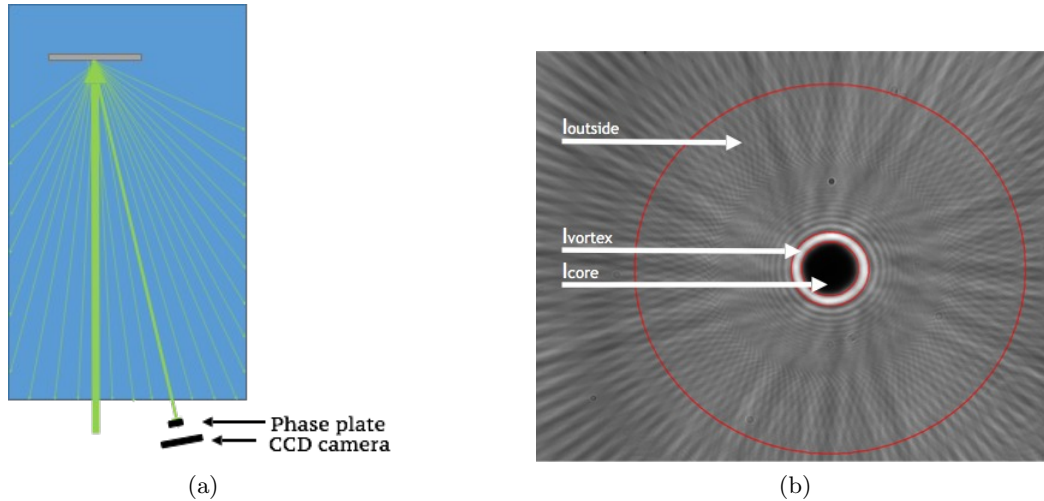


Figure 1. (a) An illustration showing the use of a spiral phase plate to analyze object-reflected light. (b) An example CCD image in clean water, showing the three regions of interest.

medium. To our knowledge though, there has been no study examining whether or not OAM is useful for these maritime applications and geometries. To this end, we report on laboratory experiments in scattering environments to study how OAM may be used for target detection in turbid water.

2. BACKGROUND

Consider the illustration in Figure 1(a) where a Gaussian beam interrogates an object in a turbid medium. Similar to the Palacios⁸ study, we use a spiral phase plate as an ‘analyzer’ and place it before a CCD camera which views the target return. As seen in the illustration, though the reflection from the object is diffuse, at any general viewing angle there exists a small fraction of rays which remain coherent to each other at the face of the spiral phase plate. These coherent ballistic rays, when passed through the phase plate, form an optical vortex while the incoherent diffuse rays do not. Therefore the phase plate acts to spatially separate the coherent and incoherent components onto different regions of the CCD camera. We can define the average intensity per pixel on three regions of the CCD camera according to the illustration in Figure 1(b) as

$$I_{vortex} = I_B \quad (1)$$

$$I_{core} = 0 \quad (2)$$

$$I_{outside} = I_D \quad (3)$$

where I_B is the coherent ballistic component and I_D is the incoherent diffuse component. The spatial pattern observed outside the vortex is believed to be due to near-field diffraction from the sections of the spiral phase plate. In turbid water, we may expect contributions from I_{bks} , the backscattered light, and I_{fwd} , the forward scattered light (scattering before or after object reflection). The three regions are then defined as,

$$I_{vortex} = I_B + I_{fwd} + I_{bks} \quad (4)$$

$$I_{core} = I_{fwd} + I_{bks} \quad (5)$$

$$I_{outside} = I_D + I_{fwd} + I_{bks} \quad (6)$$

The dependence of each of these terms on the absorption and scattering coefficients of the water is implied. The previous expressions show that there is information regarding the components of the optical return ‘embedded’ in the spatial pattern formed after passing through the phase plate ‘analyzer’. For example, the difference

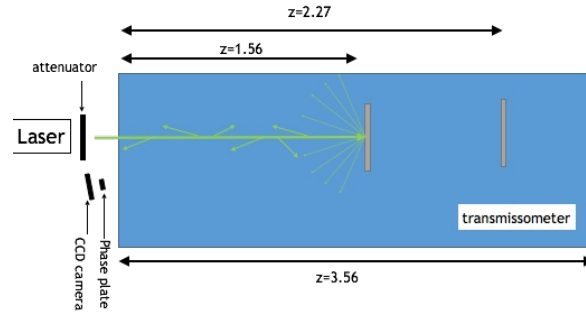


Figure 2. Experimental setup.

$I_{vortex} - I_{core}$ yields I_B , the ballistic component of the object reflected light unaffected by scattering. This suggests that coherent light from the object, though rapidly attenuating, may be recoverable even in the presence of clutter and shows how one may exploit the spatial profile to perform object discrimination.

3. EXPERIMENTAL APPROACH

The experiment was conducted in a tank that was 3.56 m long. A diode pumped solid state laser with a wavelength of 532 nm was used to illuminate a grey target. The target was placed on a motorized translation stage such that its position could be placed at one of two ranges ($z=1.56$ or $z=2.27$ m). The receiver consisted of a CCD camera with a 1.4 Megapixel resolution and an active area of 8.77 mm x 6.6 mm. A diffractive spiral phase plate ($m = 8$) was placed 9 cm in front of the camera. To align the system, the target was positioned halfway between the two target positions. A negative and positive lens focused the beam to a diameter of ~ 0.8 mm at a position halfway between target positions. Similarly, the phase plate and CCD are aligned to this halfway position such that the optical vortex was formed in the middle of the CCD active area. Though the experiment was performed in the dark, black felt was draped over the plate and camera mounts to minimize ambient light. Two transmitter/receiver separation distances, s , were considered, and the alignment procedure was repeated for each ($s=10$ and $s=25$ cm).

To alter the turbidity of the water, Equate antacid was used. This scattering agent has been previously found to closely mimic ocean conditions. A sump pump was used for the duration of the experiment to keep the antacid in suspension. An AC-9 transmissometer was used to measure the absorption and total attenuation coefficients in-situ. At each turbidity, images were taken first at the close target position ($z=1.56$ m), then the far position ($z=2.27$ m). To estimate the backscattered component, I_{bks} , a third image was obtained by removing the target from the tank completely, and averaging the intensity over the entire CCD aperture. To maintain sufficient dynamic range, the laser power was adjusted using a half wave plate and polarizer so that the camera reported approximately 80% of the digitizer saturation level. The laser power was measured using a pickoff detector and the value was recorded for each image. In post processing, the intensity of the images was scaled for changes in laser power. The camera was set to have a gain of 1 and exposure time of 1 second. To reduce small variations in between images, 5 frames were block averaged to produce each recorded image.

4. RESULTS

In post-processing, the average intensity per pixel in each of the three regions is calculated as shown in Figure 1(b). The CCD images are cropped to size, and contrast stretched according to a 0-to-max and min-to-max scheme. The minimum of the min-to-max scheme is taken from the region defined as the vortex core. Figure 3 and Figure 4 shows results with the target at $z = 1.56$ and $z = 2.27$ m respectively with the narrow transmitter/receiver separation of $s = 10$ cm. Figure 5 and Figure 6 show the same ranges, but with a wider separation of $s = 25$ cm. In all scenarios, I_{vortex} shows the greatest intensity per pixel at low turbidities, as the coherent reflection from the target dominates the return. This is confirmed by a well formed vortex as noted in the CCD images.

As scattering increases, I_{core} rises slightly and then attenuates. This is similar behavior to Palacios' study,⁸ and represents a single scattered component which increases initially, but then eventually attenuates with more

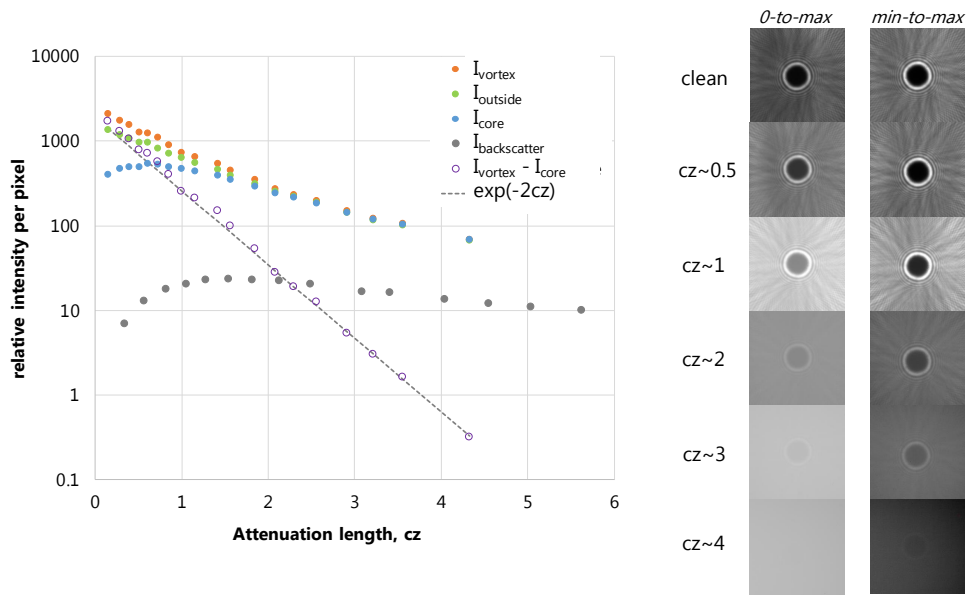


Figure 3. Target position $z = 1.56\text{m}$ and Tx/Rx separation $s = 10\text{ cm}$.

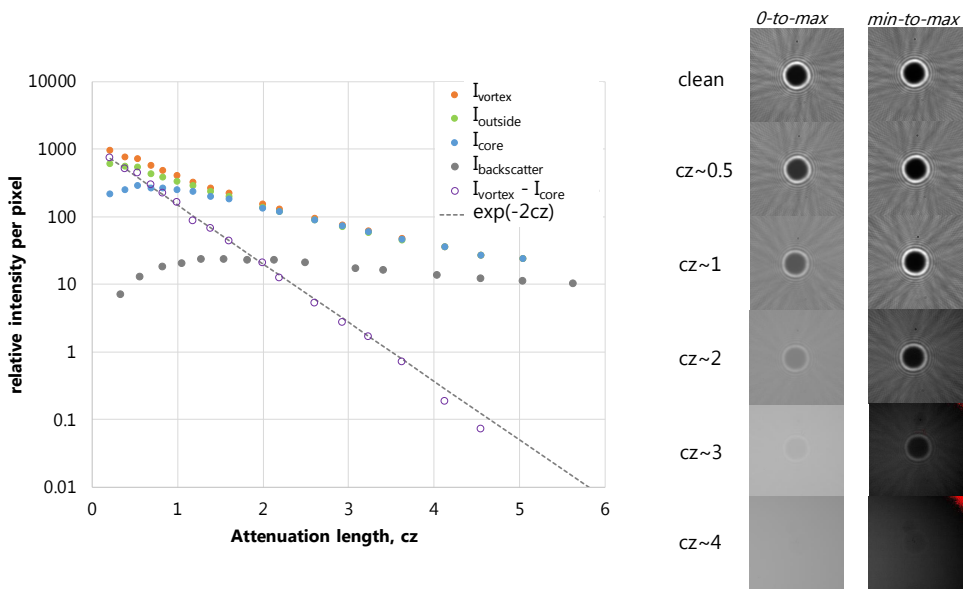


Figure 4. Target position $z = 2.27\text{m}$ and Tx/Rx separation $s = 10\text{ cm}$.

multiple scattering events. In general, the average intensity in all three regions becomes approximately equal, since the incoherent scattered components are not spatially altered when passing through the phase plate analyzer. The result is a decrease in CCD image contrast. The contrast stretched images suggest though that a coherent ballistic component, however small, does remain since a well defined vortex is still observed. Additionally, the difference ($I_{vortex} - I_{core}$) is shown to follow $exp(-2cz)$ (i.e Beer's Law for the two-way path), which suggests that a coherent object component is still present within the return. It is rather remarkable that this ballistic target return can be extracted even when its amplitude is seen to be several orders below the backscatter clutter. Furthermore, we have accomplished the detection of this small coherent signal without any complex optical heterodyning scheme, confirming our assertion that the unique properties of OAM can be exploited in order to discriminate object from environment.

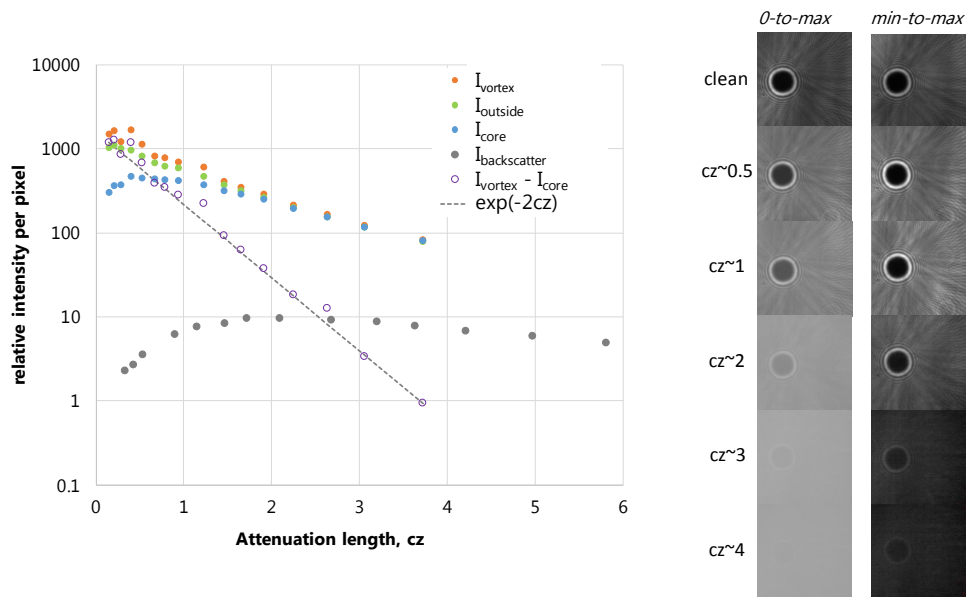


Figure 5. Target position $z = 1.56\text{m}$ and Tx/Rx separation $s = 25\text{ cm}$.

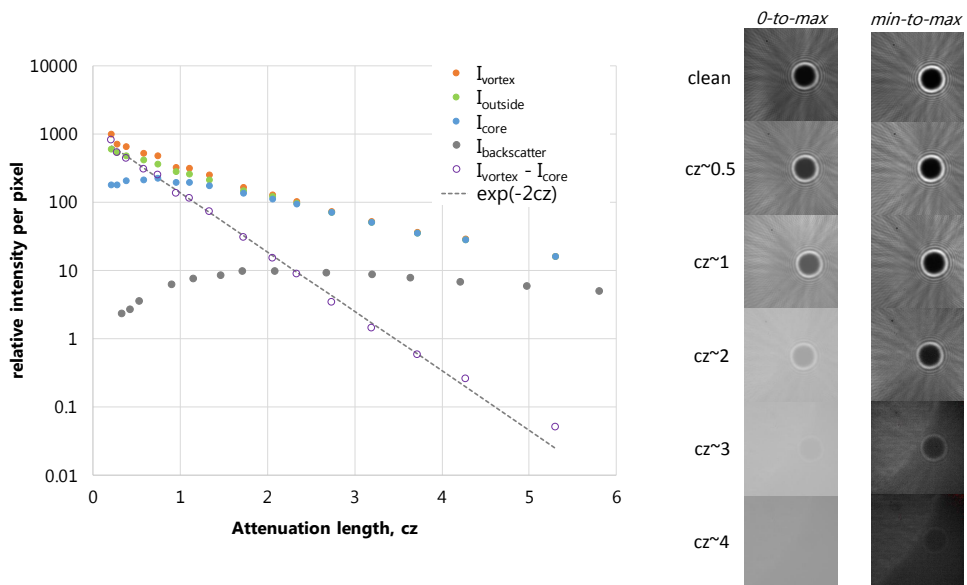


Figure 6. Target position $z = 2.27\text{m}$ and Tx/Rx separation $s = 25\text{ cm}$.

5. CONCLUSIONS AND FUTURE WORK

We have presented initial experiments that suggest OAM can be used as an analyzer for the optical detection of objects in a turbid underwater medium. This is achieved by exploiting the spatial relationships of coherent and incoherent light after it passes through a spiral phase plate. While we have shown that the object signal may be recovered over a modest amount of attenuation lengths, there are still several outstanding questions that warrant future study. Namely, the current method provides no way of observing how the vortex evolves as photons traverse the medium (i.e. over time). Using a pulsed laser and fast receiver however would allow for this time-resolved measurement of the spatial intensity pattern. Future experiments are planned to better understand how both temporal and spatial discrimination can be used together to enhance detection.

ACKNOWLEDGMENTS

This work is supported by the Office of Naval Research, Code 32.

REFERENCES

- [1] Allen, L., Beijersbergen, M. W., Spreeuw, R. J. C., and Woerdman, J. P., "Orbital angular momentum of light and the transformation of Laguerre-Gaussian laser modes," *Physical Review A* **45**, 8185–8189 (June 1992).
- [2] Baghdady, J., Miller, K., Morgan, K., Byrd, M., Osler, S., Ragusa, R., Li, W., Cochenour, B. M., and Johnson, E. G., "Multi-gigabit/s underwater optical communication link using orbital angular momentum multiplexing," *Optics Express* **24**, 9794–9805 (May 2016).
- [3] Baghdady, J., Miller, K., Osler, S., Morgan, K., Li, W., Johnson, E., and Cochenour, B., "Blue-light digital communication in underwater environments utilizing orbital angular momentum," in [*Proc of SPIE*], Hou, W. W. and Arnone, R. A., eds., 98270G–98270G–8, International Society for Optics and Photonics (May 2016).
- [4] Cochenour, B., Morgan, K., Miller, K., Johnson, E., Dunn, K., and Mullen, L., "Propagation of modulated optical beams carrying orbital angular momentum in turbid water," *Applied Optics* **55**, C34–C38 (Nov. 2016).
- [5] Sun, W., Hu, Y., MacDonnell, D. G., Weimer, C., and Baize, R. R., "Technique to separate lidar signal and sunlight," *Optics Express* **24**(12), 12949–6 (2016).
- [6] Foo, G., Palacios, D. M., and Swartzlander, G. A., "Optical vortex coronagraph," *Optics Letters* **30**, 3308–3310 (Dec. 2005).
- [7] Swartzlander Jr, G. A., Ford, E. L., Abdul-Malik, R. S., Close, L. M., Peters, M. A., Palacios, D. M., and Wilson, D. W., "Astronomical demonstration of an optical vortex coronagraph," *Optics Express* **16**(14), 10200–10207 (2008).
- [8] Palacios, D., Rozas, D., and Swartzlander, G. A., "Observed Scattering into a Dark Optical Vortex Core," *Physical Review Letters* **88**, 103902–4 (Mar. 2002).
- [9] Beijersbergen, M. W., Coerwinkel, R. P. C., Kristensen, M., and Woerdman, J. P., "Helical-wavefront laser beams produced with a spiral phaseplate," *Optics Communications* **112**, 321–327 (Dec. 1994).